IMPACT OF TIGHT HORIZONTAL LAYERS ON DISSOLUTION TRAPPING IN GEOLOGICAL CARBON STORAGE

Maria T. Elenius and Sarah E. Gasda

Uni Research
Centre for Integrated Petroleum Research
PO Box 7800, 5020 Bergen, Norway
e-mail: maria.elenius@uni.no, sarah.gasda@uni.no, web page: `http://www.cipr.uni.no/`

Key words: CO_2 storage, porous media, convection, heterogeneity

Summary. We show that tight horizontal layers reduce the efficiency of CO_2 dissolution in geological CO_2 storage. The efficiency is reduced exponentially with enhanced layer extent.

1 INTRODUCTION

As a method to reduce atmospheric emissions of carbon dioxide (CO_2), this greenhouse gas can be separated at large point-sources, compressed and injected into geological formations such as saline aquifers. Several physical features of the fluids and the rock sequester the CO_2 in the pores of the rock for geologic time-scales. One such feature is dissolution into the brine, which increases the density of the brine and thereby reduces the risk of upward migration. This is referred to as dissolution trapping, and it is often an important trapping mechanism[1–3].

The efficiency of dissolution trapping is largely due to density-driven convective mixing. Convective mixing of dissolved CO_2 has been studied in homogeneous systems (e.g.[4,5]). All real storage formations are heterogeneous in permeability and porosity and this may affect the efficiency. Farjazadeh et al.[6] studied the effect of random heterogeneity fields. In their simulations they found that heterogeneity implied enhanced dissolution rates compared with the homogeneous case. Green et al.[7] showed that the dissolution rate in an aquifer with horizontal low-permeability layers of small lateral extent can be modelled approximately based on an anisotropic permeability that uses the effective vertical permeability. Post and Simmons[8] studied the effect of low-permeability layers of larger extent on sequestration of a solute (salt in their case) in the low-permeability strata, but they did not focus on the overall dissolution. The efficiency of CO_2 dissolution trapping in systems with large low-permeability structures is therefore still largely unknown.

In this paper, we perform numerical simulations to investigate the efficiency of CO_2-dissolution in aquifers with tight horizontal layers of extent larger than the intrinsic wave-

length of unstable fingers. As an example, these layers could be thin shale deposits or mudstone inclusions in sandstone aquifers.

2 MODEL PROBLEM AND NUMERICAL TREATMENT

We focus on the effect of tight layers on the redistribution of a solute (e.g. CO_2) within the water phase, considering that there is a source (e.g. a CO_2 plume) along the top boundary of the domain. The problem is modelled by Darcy's law, a transport equation for the solute, the Boussinesq approximation and a linear density dependence on concentration:

$$\mathbf{u} = -\frac{K}{\mu}(\nabla P - \rho\mathbf{g}), \tag{1}$$

$$\phi\,\partial_t c = -\mathbf{u}\cdot\nabla c + \phi D\nabla^2 c, \tag{2}$$

$$\nabla\cdot\mathbf{u} = 0, \tag{3}$$

$$\rho = \rho_0 + \Delta\rho c. \tag{4}$$

Here, $\mathbf{u}$ denotes the Darcy velocity, K the permeability, μ the viscosity, P the pressure, $\mathbf{g}$ the vector of gravity, ϕ the porosity, D the diffusion coefficient, ρ_0 the minimum density and $\Delta\rho$ the maximum density difference induced by the solute. The concentration c is scaled to values between 0 and 1. The tight layers are modelled as internal no-flow boundary conditions and hence we do not solve the equations within those regions. All properties therefore refer to the (homogeneous) aquifer surrounding the layers. The equations are scaled by the characteristic velocity $u_c = K\Delta\rho g/\mu$, length $l_c = D\phi/u_c$ and time $t_c = D\phi^2/u_c^2$. In addition, the nondimensional pressure p is related to P by $P = D\mu\phi/K(p + \rho_0/\Delta\rho\,z)$. The non-dimensional form of the equations is:

$$\mathbf{u} = -(\nabla p - c\mathbf{e_z}), \tag{5}$$

$$\partial_t c = -\mathbf{u}\cdot\nabla c + \nabla^2 c, \tag{6}$$

$$\nabla\cdot\mathbf{u} = 0. \tag{7}$$

The choice of representing the shale layers as no-flow regions is an approximation of the real system. Given the large contrast between permeability and porosity in e.g. sandstone and shale, flow through layers is likely to be small. In addition, our choice facilitates comparison with analytical models, and is helpful for understanding the dissolution based solely on the geometric properties of the layers, which is our focus.

The boundary conditions and schematic layer geometry are described in Figure 1 for our two-dimensional setting. The constant concentration top boundary condition approximates the dissolution of CO_2 from the plume above the domain. Initially, the concentration within the domain is zero and the fluid is stagnant, apart from small random perturbations $c(x, z, 0) \in [-10^{-6}, 10^{-6}]$ on the first grid nodes below the top boundary and associated perturbations in the pressure and flux field by equations (5)-(7). The onset
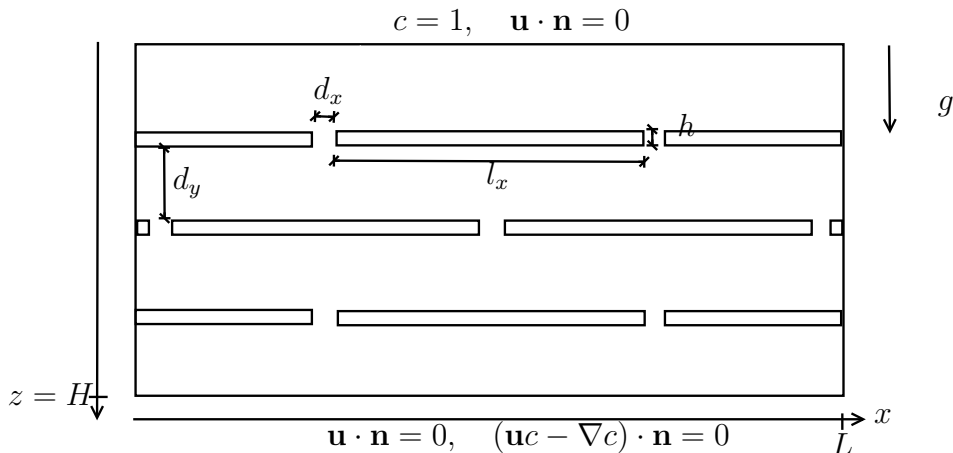
Figure 1: Nondimensional model domain, including sample thin low-permeability layers, and boundary conditions. The bottom boundary condition (no-flow) is also applied for the side boundaries and for the layers. The solute source above the model domain is modelled by a constant concentration, and advective exchange with the source (e.g. a two-phase region) is neglected here for simplicity, although it can affect the dissolution rate[9].

time of enhanced dissolution (the "nonlinear onset time") depends on the size of initial perturbations[5] and is not the current focus.

The problem is solved using numerical simulations with the software d^3f [10,11]. The governing equations are discretized in time with a second order two-step diagonal implicit Runge-Kutta scheme (the Alexander scheme). The control volume finite element method is used, where the variables are located at the nodes. Furthermore, we apply the second order central difference scheme for space discretization. The nonlinear system is solved with Newton's method and the linear sub-problems are solved with the biconjugate gradient stabilized method (BiCGSTAB), with a multigrid preconditioner and overlapping block Gauss-Seidel smoother. We used cells of nondimensional size 62.5 x 62.5 and a constant nondimensional time-step size 1000, apart from a couple of temporary time-step reductions for the homogeneous reference case. With these choices, reasonable finger shapes and behavior is obtained at late times, which is our focus. We vary l_x between 500 and 4000 and also compare with a domain that has no layers.

3 RESULTS

From Figure 2 we observe that increasing shale length dampens the downward component of flow. In addition, the horizontal wavelength of "fingers" becomes enhanced due to the lateral dispersion caused by the layers. It is probable that the chosen configuration leads to a worst-case scenario for any given shale length, since the openings are symmetrically staggered in the vertical.

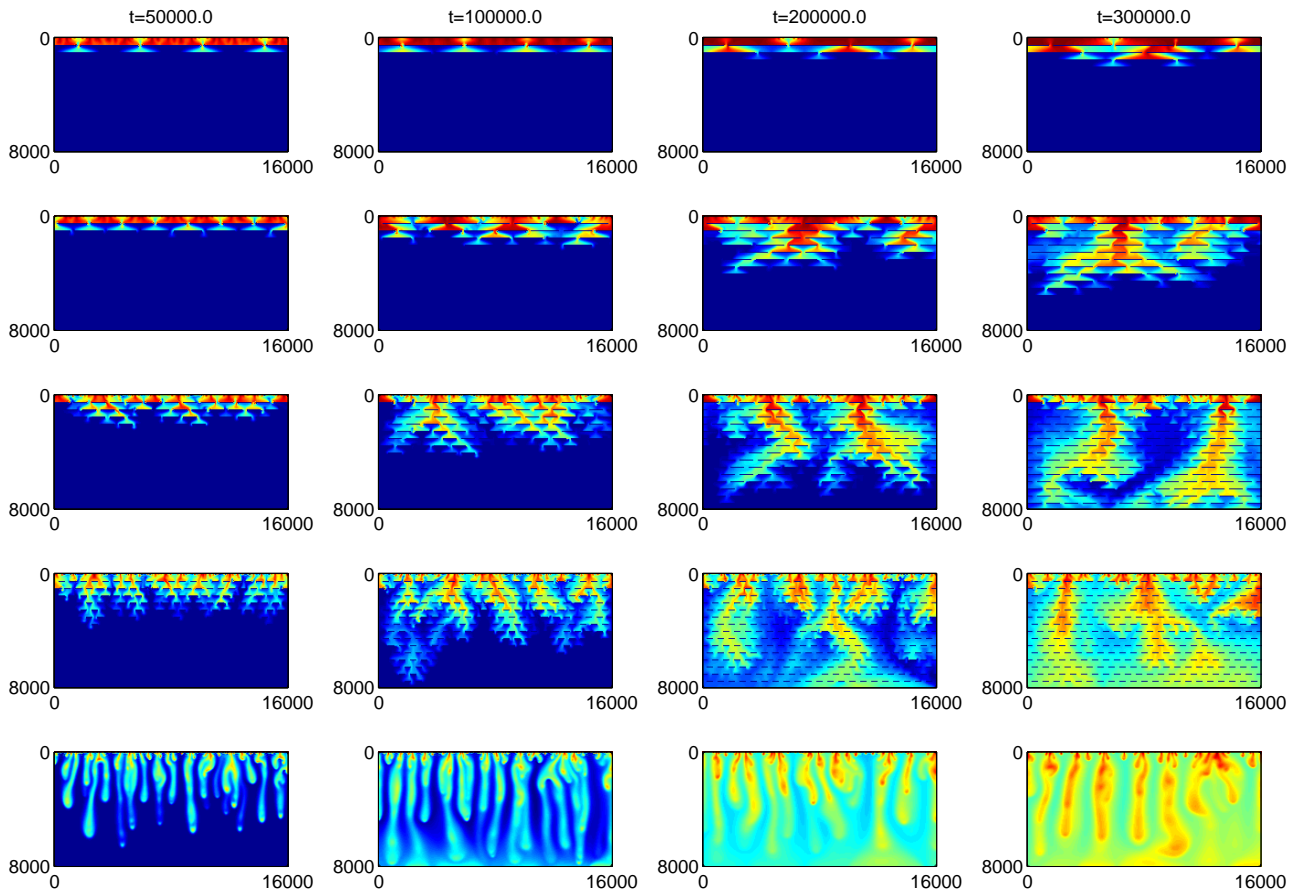In each case, the first (top) high-permeability zone (HPZ) fills up and CO_2 enters

3

Figure 2: Concentration of CO_2 in aquifers that have tight layers of different lengths, from the top: $l_x = 4000$, $l_x = 2000$, $l_x = 1000$, $l_x = 500$ and $l_x = 0$. Dark red is (scaled) concentration 1 and dark blue is concentration 0.

through the openings to the second HPZ. Initially, in each horizontal opening between layers, there is counter-current flow and the shape of the iso-concentration lines resembles the shape of iso-saturation lines obtained by Hesse and Woods[12] for two-phase flow in a layered medium.

Let us examine the $l_x = 2000$ case (second from the top) more closely. At $t = 50000$, dissolved CO_2 has a symmetric distribution and has started to spill over to the third HPZ. At $t = 100000$ it is clear that the flow is no longer symmetric. Some fingers have merged, and now the flow is directed downward through some openings and upward through other openings. It is possible that symmetric flow could prevail for longer times if the horizontal openings were larger. At $t = 200000$ and $t = 300000$ we also notice that the wavelength (finger width) is smallest deep in the domain, at the advancing "tip(s)".

The depth of the tip as a function of time is shown in Figure 3a. Again, we notice that larger layer extent gives slower tip propagation, and it is also clear that the tip speed is approximately constant between the time when the third HPZ is entered and the time when the bottom of the domain is reached (or the end of simulation if the bottom is not reached). However, for short time-intervals, the downward speed varies between zero when the concentration front moves horizontally along a layer, and a larger value when dissolved CO_2 migrates down to the next layer. It naturally takes a longer time for the CO_2 to travel along layers to the next opening when the layers are large, but in addition, the migration speed to the next layer is reduced in these cases. The slower downward flow with large layers reduces the efficiency of dissolution trapping, as shown in Figure 3b for the mass of dissolved CO_2, and in Figure 3c for the dissolution rate. The mass is here defined as the concentration multiplied by the volume under a unit area of the top boundary (all nondimensional), and the dissolution rate is the time-derivative of this mass. Until the time when the bottom boundary is reached, this definition of dissolution rate is invariant to the thickness of the domain.

In Figures 4a and 4b, the average tip speed and dissolution rate are shown as functions of l_x. Note that the vertical scale (only) is logarithmic and that the lines are approximately linear (apart from the $l_x = 500$ and $l_x = 0$ cases for the finger speed). Therefore, it appears that the finger speed and dissolution rate are exponential functions of l_x.

4 DISCUSSION AND CONCLUSIONS

We investigated the efficiency of dissolution trapping in the presence of horizontal shale layers. The exact dissolution rates may differ in 3D compared to our 2D approximation, and although finger shapes look reasonable, we have not yet performed a study of numerical errors and sample variation. However, our results clearly show that horizontal tight layers significantly reduce the dissolution rates, as opposed to the random heterogeneity investigated by Farjazadeh et al[6], and this effect is increasing exponentially with the layer extent. This may impact the efficiency of dissolution trapping, especially for extensive layers. The flow pattern is complicated, with downward flow through some openings and upward flow through other openings. Therefore, it does not seem that a purely analyt-
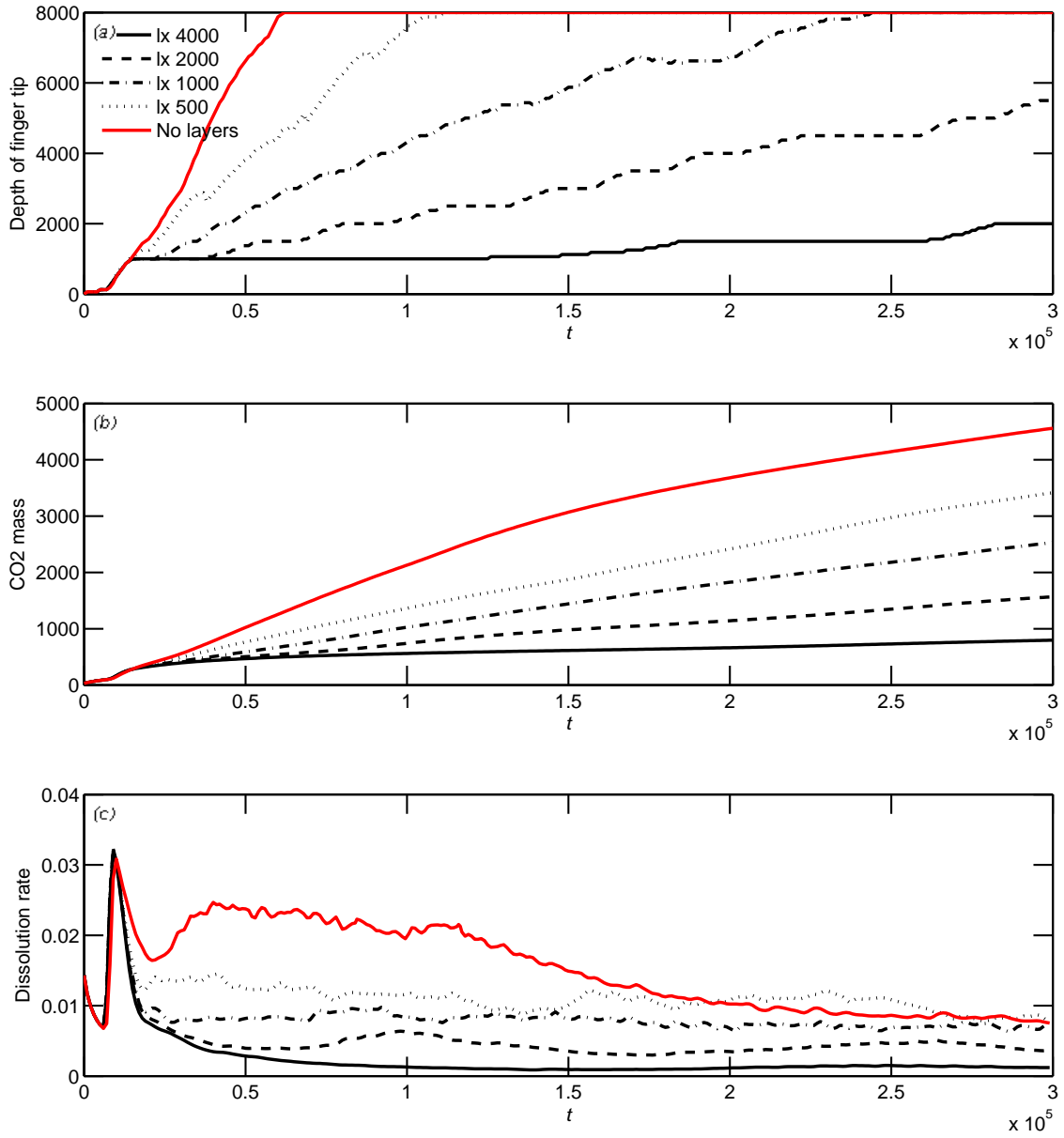
5

Figure 3: *a*) Depth of the finger tip defined as the lowest occurrence the concentration $c = 0.2$, *b*) Mass of CO_2 in the domain per unit length of the upper boundary, and *c*) Dissolution rate, i.e. the mass flux into the domain per unit length of the top boundary. All variables are nondimensional as explained in the text.
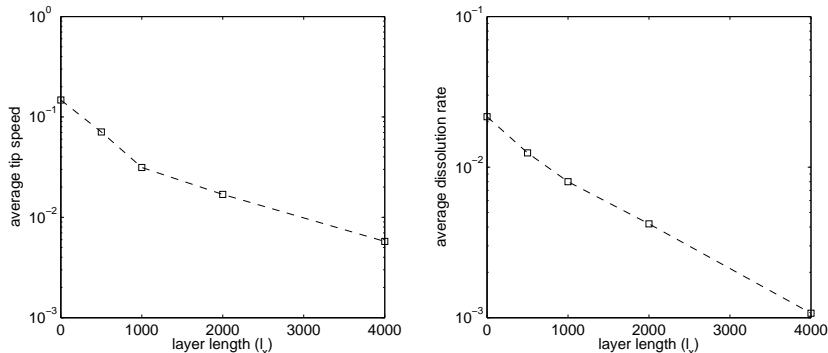
Figure 4: *a*) Average tip speed and *b*) Average dissolution rate. These averages are calculated for the time interval that has most stable speed, from the time when the finger tip is located at a small distance (100) into the third HPZ and the time when the finger tip reaches the bottom of the domain (or if the fingers do not reach the bottom, we chose end time as the end time of simulation), cf. Figure 3.

ical approach would predict the flow and dissolution efficiency. However, it seems that extrapolation of our results can be made to layers of larger extent, which may be difficult to study numerically.

We performed the investigation in a nondimensional setting in order to obtain results applicable for different storage sites. Here, we apply the results to the Utsira formation in the North Sea, where CO_2 has been injected since 1996. Using parameters from the literature for the formation and fluids, as summarized by Elenius and Johannsen[5], dimensional time is obtained by multiplication of the nondimensional times with $t_c = 7.3 \cdot 10^{-5}$ years, and similarly, dimensional length scales are obtained by multiplication with $l_c = 0.0015$ m, and dissolution rate by multiplication with $F_c = 420$ kg/(m^2 year). Therefore, the domain is 24 m wide and 12 m deep, and shale layers of $l_x = 2000$ have dimensional length 3 m. The total simulation period is 22 years, and the tip speed with these 3 m - shales as defined above is 0.3 m/year (a reduction by a factor 10 from the homogeneous case). The dissolution rate depends on the interface area between the plume and water, which is changing in time as $A(t) = 2t/3 \cdot 10^6$ m^2 (our simplified formulae based on data presented by[13]). The dissolution since 1996 is then estimated as 2 % of all injected CO_2, compared to 10 % in the homogeneous case. Here, we have neglected advective interaction between convection and the plume which may considerably enhance the dissolution rates[9]. Many CO_2 storage sites have lower permeability, which leads to larger dimensional time- and length-scales and smaller dissolution rates compared to the Utsira formation.

5   ACKNOWLEDGEMENT

References

[1] Elenius, M., Tchelepi, H., and Johannsen, K. CO_2 trapping in sloping aquifers: High resolution numerical simulations. *XVIII International Conference on Water Resources* (2010).

[2] Gasda, S., Nordbotten, J., and Celia, M. Application of simplified models to CO_2 migration and immobilization in large-scale geological systems. *Int. J. Greenhouse Gas Control* (Under review).

[3] Gasda, S., Nordbotten, J., and Celia, M. Vertically averaged approaches for CO_2 migration with solubility trapping. *Water Resour. Research* **47** (2011).

[4] Riaz, A., Hesse, M., Tchelepi, H., and Orr, F. Onset of convection in a gravitationally unstable diffusive boundary layer in porous media. *J. Fluid Mech.* **548**, 87–111 (2006).

[5] Elenius, M. and Johannsen, K. On the time scales of non-linear instability in miscible displacement porous media flow. *Computational Geosciences* (Under review).

[6] Farjazadeh, R., Ranganathan, P., Zitha, P., and Bruining, J. The effect of heterogeneity on the character of density-driven natural convection of CO_2 overlying a brine layer. *Adv. Water. Resour.* **34**, 327–339 (2011).

[7] Green, C., Ennis-King, J., and Pruess, K. Effect of vertical heterogeneity on long-term migration of CO_2 in saline formations. *Energy Procedia* **1**, 1823–1830 (2009).

[8] Post, V. and Simmons, C. Free convective controls on sequestration of salts into low-permeability strata: insights from sand tank laboratory experiments and numerical modelling. *Hydrogeology Journal* **18**, 39–54 (2010).

[9] Elenius, M., Nordbotten, J., and Kalisch, H. Effects of a capillary transition zone on the stability of a diffusive boundary layer. *IMA J. Appl. Math.* (Accepted for publication).

[10] Fein, E. d^3f-Ein Programmpaket zur Modellierung von Dichteströmungen. *GRS, Braunschweig, GRS-139* (1998).

[11] Johannsen, K. Numerische Aspekte dichtegetriebener Strömung in porösen Medien. *Professorial dissertation (habilitation), Heidelberg, Germany* (2004).

[12] Hesse, M. and Woods, A. Buoyant dispersal of CO_2 during geological storage. *Geophys. Res. Lett.* **37** (2010).

[13] Boait, F., White, N., Chadwick, A., Noy, D., and Bickle, M. Layer spreading and dimming within the CO_2 plume at the Sleipner Field in the North Sea. *Energy Proceedia* **4**, 3254–3261 (2011).